ApJL, Accepted July 3, 2014
Preprint typeset using LaTeX style emulateapj v. 5/2/11

arXiv:1406.4413v2 [astro-ph.GA] 8 Jul 2014

LINKING Lyα AND LOW-IONIZATION TRANSITIONS AT LOW OPTICAL DEPTH

A. E. Jaskot and M. S. Oey
University of Michigan, Department of Astronomy, 830 Dennison Building, Ann Arbor, MI 48109, USA.
ApJL, Accepted July 3, 2014

ABSTRACT

We suggest that low optical depth in the Lyman continuum (LyC) may relate the Lyα emission, C II and Si II absorption, and C II* and Si II* emission seen in high-redshift galaxies. We base this analysis on *Hubble Space Telescope* COS spectra of four Green Pea (GP) galaxies, which may be analogs of $z > 2$ Lyα emitters (LAEs). In the two GPs with the strongest Lyα emission, the Lyα line profiles show reduced signs of resonant scattering. Instead, the Lyα profiles resemble the Hα line profiles of evolved star ejecta, suggesting that the Lyα emission originates from a low column density and similar outflow geometry. The weak C II absorption and presence of non-resonant C II* emission in these GPs support this interpretation and imply a low LyC optical depth along the line of sight. In two additional GPs, weak Lyα emission and strong C II absorption suggest a higher optical depth. These two GPs differ in their Lyα profile shapes and C II* emission strengths, however, indicating different inclinations of the outflows to our line of sight. With these four GPs as examples, we explain the observed trends linking Lyα, C II, and C II* in stacked LAE spectra, in the context of optical depth and geometric effects. Specifically, in some galaxies with strong Lyα emission, a low LyC optical depth may allow Lyα to escape with reduced scattering. Furthermore, C II absorption, C II* emission, and Lyα profile shape can reveal the optical depth, constrain the orientation of neutral outflows in LAEs, and identify candidate LyC emitters.

Subject headings: Galaxies: high-redshift — Galaxies: starburst — Intergalactic medium — Line: profiles — Radiative transfer — Ultraviolet: ISM

1. INTRODUCTION

Lyman continuum (LyC) radiation from star-forming galaxies likely caused the reionization of the universe (e.g., Bouwens et al. 2012), but to date, studies have identified few galaxies that are LyC emitters (LCEs; e.g., Leitherer et al. 1995; Heckman et al. 2001; Leitet et al. 2013; Nestor et al. 2013). At low redshift, the Green Pea (GP) galaxies, starbursts characterized by intense [O III] λ5007 emission, have emerged as LCE candidates (Jaskot & Oey 2013; Verhamme et al. 2014, hereafter V14). The high [O III]λ5007/[O II]λ3727 ratios of the GPs imply an extreme ionization parameter. However, since optically thin nebulae should underproduce [O II] (e.g., Giammanco et al. 2005; Pellegrini et al. 2012), these high ratios may also indicate a low LyC optical depth. Notably, the $z < 0.3$ GPs share several properties with Lyα emitters (LAEs) at $z > 2$, including high specific star formation rates, compact sizes, low extinction, and elevated [O III]/[O II] ratios (e.g., Hagen et al. 2014; Malhotra et al. 2012; Gawiser et al. 2007; Nakajima & Ouchi 2013). Thus, the GPs may be outstanding analogs of both high-redshift LyC-emitting and Lyα-emitting galaxies.

Some LAEs are known LCEs (e.g., Iwata et al. 2009; Nestor et al. 2013, but see Vanzella et al. 2010), and several studies have proposed a connection between Lyα emission and a low LyC optical depth (e.g., Shapley et al. 2003; Nakajima & Ouchi 2013; V14). Due to the resonant nature of Lyα, most galaxies have low Lyα escape fractions (e.g., Hayes et al. 2011). The geometry and kinematics of the neutral interstellar medium (ISM) appear to control the Lyα escape fraction (e.g., Giavalisco et al. 1996; Thuan & Izotov 1997; Kunth et al. 1998), with low neutral gas covering fractions and strong outflows enabling Lyα escape (e.g., Shapley et al. 2003; Kornei et al. 2010). While many numerical models have considered the effects of strong scattering through the ISM or outflows on Lyα line profiles (e.g., Ahn et al. 2000; Zheng & Miralda-Escudé 2002; Verhamme et al. 2006; Orsi et al. 2012), recent studies have focused on Lyα radiative transfer through an optically thin medium (Behrens et al. 2014; V14). By driving outflows and ionizing the surrounding ISM and circumgalactic medium, feedback from the intense star formation in some galaxies, like the GPs, may create optically thin conditions that enable LyC and Lyα escape.

In this *Letter*, we suggest that LyC optical depth and outflow geometry link the Lyα profiles, C II absorption, and C II* emission observed in high-redshift galaxies. We demonstrate this connection using *Hubble Space Telescope (HST)* Cosmic Origins Spectrograph (COS) observations of four of the most extreme GPs, galaxies that closely resemble high-redshift LAEs. We report the detection of Lyα emission in all four GPs. Three GPs show P-Cygni Lyα line profiles; the profile shapes and equivalent widths (EWs) > 70 Å in two GPs imply a relatively low optical depth. We also suggest that the enigmatic non-resonant emission in C II* and Si II* that is observed to correlate with Lyα emission from starbursts is consistent with the geometry, optical depth, and viewing orientation associated with the GPs' galactic outflows. We will show that the Lyα emission strengths, Lyα profile shapes, and weak interstellar absorption lines in two GPs demonstrate that some starbursts with high [O III]/[O II] may be optically thin to the LyC.

2. RESULTS

We present *HST* COS spectra of two GPs (J081552.00+215623.6 and J145735.13+223201.8) and analyze archival observations for two additional GPs (J121903.98+152608.5 and J030321.41-075923.2). Jaskot & Oey (2013) identify these four starbursts as LCE candidates due to their high [O III]/[O II] ratios. All four GPs have similar optical spectra, metallicities ($\sim 0.2\,Z_\odot$), extinctions ($E(B-V) = 0.06 - 0.11$), and young ages (Hα EW= $700 - 1300$ Å), but differ markedly in their UV spectra (Figures 1 and 2; Table 1). We bin the COS spectra to $0.15 - 0.23$ Å per pixel, the resolution for emission at the GPs' NUV half-light radii (Table 1), as measured from the COS acquisition images (e.g., James et al., in prep). Galactic Si II λ1526.71 absorption lines show that the wavelength scale is accurate to within one binned pixel. At the GPs' redshifts, the COS aperture samples 6-8 kpc and fully encompasses the detected NUV emission. However, Lyα emission may originate at larger radii (e.g., Hayes et al. 2013). Based on the GPs' NUV Petrosian radii (Petrosian 1976) at the $\eta = 0.2$ surface brightness level and the average ratio of Lyα radii to FUV radii in Hayes et al. (2013), we expect the COS aperture to capture all of the Lyα emission. Even adopting the ratio for the most extended Lyα halo in Hayes et al. (2013), the COS aperture should probe $60 - 100\%$ of the Lyα Petrosian radius and recover most of the Lyα flux. We use the redshifts given in the Sloan Digital Sky Survey (SDSS) Data Release 9 (Ahn et al. 2012), which are based on the GPs' optical emission lines. We adopt a cosmology with $H_0 = 70$ km s^{-1} Mpc^{-1}, $\Omega_m = 0.3$, and $\Lambda_0 = 0.7$.

2.1. *Lyα Emission*

In the conventional scenario for Lyα emission, Lyα scatters many times before escaping, which significantly alters and broadens the original line profile. However, the Lyα profiles in the two GPs with the highest [O III]/[O II] ratios, J0816+22 and J1219+15, do not show the predicted effects of radiative transfer at high column density. The Lyα profiles in these two GPs resemble a Gaussian with P Cygni-like absorption superimposed at the systemic velocity; both galaxies have a small separation (<300 km s^{-1}) of the Lyα peaks, (Figure 1), as expected for a neutral column density $N_{\rm HI} < 10^{18}$ cm^{-2} and optical depth at the Lyman edge $\tau \lesssim 6$ (V14). Indeed, V14 note that a density-bounded scenario could explain the Lyα profile of J1219+15.

In contrast, the Lyα profiles in the other two GPs, J0303-08 and J1457+22, are consistent with higher Lyα optical depths. J0303-08 exhibits a classic P-Cygni profile, with deeper, blue-shifted absorption, a weaker blue peak, and a greater separation of the emission peaks (Figure 1c) than J0816+22 and J1219+15, implying a higher optical depth. This GP appears slightly more extended than the others and consists of multiple UV-emitting knots; thus, the COS aperture may miss some of the scattered emission. J1457+22 appears to have the highest line-of-sight column density, as indicated by the $\sim$750 km s^{-1} velocity separation of its emission peaks and the broad absorption trough extending to either side of the Lyα emission (Figure 1d). The weak, double-peaked profile of J1457+22 resembles models of Lyα emission from highly inclined galaxies (Verhamme et al. 2012).

The P-Cygni Lyα profiles of J0816+22, J1219+15, and J0303-08 are strikingly similar to Hα emission line profiles observed from stellar sources, such as symbiotic binaries (e.g., Fig. 4 of Burmeister & Leedjärv 2009) and luminous blue variables (LBVs; e.g., Fig. 4 of Weis 2003). Double-peaked Hα emission lines with weakly blue-shifted absorption are particularly common in symbiotic binaries (e.g., Quiroga et al. 2002; Burmeister & Leedjärv 2009), which consist of a hot compact star interacting with the wind of a red giant. The Hα emission forms in the gas ionized by the hot star, while self-absorption from neutral gas in the red giant's wind may cause the central absorption dip (e.g., Ivison et al. 1994; Quiroga et al. 2002). Similar Balmer line profiles arise in LBVs (e.g., Nota et al. 1997; Weis 2003) and proto-planetary nebulae (e.g., Balick 1989; Sánchez Contreras et al. 2008). In each of these cases, photons from an expanding ionized region or bipolar outflow encounter cooler surrounding material, often ejected by the central object.

The narrow line profiles of J0816+22 and J1219+15 suggest a lower-than-average Lyα optical depth and possible LyC escape. In addition, the Lyα profiles' resemblance to the Balmer line profiles of stellar sources indicates that they may originate from a similar geometry, with a thin layer of neutral hydrogen obscuring a compact ionizing source. As a resonant transition, Lyα photons generally experience numerous scatterings. In contrast, the similarity of the GPs' Lyα to emission profiles from a *non-resonant* transition argues that Lyα is escaping relatively unimpeded from these objects, with a reduced number of scatterings.

To illustrate this point, we estimate the intrinsic Lyα profiles of J0816+22 and J1219+15 from their SDSS Hα profiles (Figure 3) scaled by the Case B Lyα/Hα ratio of 8.7 (Brocklehurst 1971). The Lyα emission wings extend beyond the estimated intrinsic profiles, suggesting scattered emission. Similarly, scattering likely causes the broad Hα wings in symbiotic star spectra (e.g., Lee 2000). The Lyα profile still preserves the signature of the intrinsic emission, however, and the Lyα peaks are located near or within the intrinsic profile. In Figure 4, we neglect the central absorption and fit the Lyα emission of J0816+22 and J1219+15 with a two-component sum of Gaussian functions or with a Voigt profile. Based on the adjusted R^2 goodness-of-fit statistic, these models are preferable to a single Gaussian fit, although the improvement is marginal for J0816+22. The narrow components of the double-Gaussian fits have FWHM values of 280 km s^{-1} for J0816+22 and 220 km s^{-1} for J1219+15 and the Gaussian components of the Voigt fits have FWHM=230 km s^{-1} and 100 km s^{-1} respectively. These velocities are similar to the FWHM of the Hα profiles: 180 km s^{-1} for J0816+22 and 150 km s^{-1} for J1219+15 although these widths are upper limits given the $\sim$150 km s^{-1} SDSS spectral resolution. The narrow peak separations and presence of narrow emission components suggest that Lyα photons do not need to scatter to high velocities in order to escape. In addition, the strength of the blue peak indicates that this escape is due to a low column density rather than a high velocity outflow (V14).

A low line-of-sight optical depth is consistent with

the high strength of the Lyα emission in J0816+22 and J1219+15. These two GPs have rest-frame EWs of $\sim$70 Å and 150 Å and Lyα escape fractions of 19% and 37%, with our assumed Lyα/Hα ratio of 8.7. Such high EWs are rare at low redshift (e.g., Finkelstein et al. 2009; Cowie et al. 2010), but fall in the range for LAEs at $z = 3$ (e.g., Ciardullo et al. 2012). J0303-08 has weaker Lyα emission with an EW$\approx$10 Å and Lyα escape fraction of 2%, consistent with its higher optical depth. As expected, the Lyα emission of J1457+22 is the weakest, with an escape fraction of < 1%.

2.2. *Interstellar Absorption and Emission Lines*

In stacked spectra of $z > 2$ LAEs, the strength of non-resonant emission lines such as Si II* and C II* appears to correlate with Lyα strength (e.g., Shapley et al. 2003; Berry et al. 2012). The origin of these lines is debated (e.g., Shapley et al. 2003; Erb et al. 2010; Berry et al. 2012), but here, we suggest that they probe the neutral ISM optical depth and geometry. In particular, for the GPs, the behavior of this emission supports the optical depths suggested by the Lyα profiles.

The non-resonant C II* λ1335.7 and Si II* λ1264.7 emission lines form when an excited electron decays to the first fine-structure level above the ground state. These lines share the same upper level as the C II λ1334.5 and Si II λ1260.4 resonant transitions, which appear in absorption in stacked LAE spectra (e.g., Shapley et al. 2003). Since these absorption lines arise in the neutral ISM, their optical depths are related to the LyC optical depth and the ISM metallicity (e.g., Heckman et al. 2001), and they offer an indirect diagnostic of the line-of-sight (LOS) optical depth.

J0816+22 and J1219+15 show no detectable C II or Si II absorption, consistent with a low optical depth (Figure 2). As seen in spectra of high-redshift LAEs, both GPs show C II* and possible Si II* emission. In contrast, J0303-08 and J1457+22 have clear absorption in C II and Si II. The absorption in J0303-08 is broad and blueshifted, implying the presence of an outflow, while the narrow emission and absorption in J1457+22 originate from a relatively static absorbing column. The width of the absorption lines in J0303-08 is not due to a lower spectral resolution, since the C II and Si II absorption lines are four times wider than the observed Milky Way Si II absorption. J0303-08 also has the lowest metallicity of the four galaxies (Izotov et al. 2011), which implies that the relative absorption strengths in the GPs do not result solely from metallicity effects. J0303-08 and J1457+22 do differ in their C II* emission, however. While J0303-08 does not have clear C II* emission, J1457+22 exhibits the strongest C II* emission of the four GPs. We summarize the spectral line strengths of the GPs in Table 1. In the following discussion, we refer to C II, but the results are equally applicable to Si II.

Models for Fe II transitions developed by Prochaska et al. (2011) suggest an interpretation of the C II* emission that is entirely consistent with the geometries and optical depths implied by the GPs' Lyα emission and ISM absorption lines. Like Fe II λ2586 and Fe II* λ2612, the non-resonant C II* and Si II* transitions have a slightly higher transition probability than the corresponding C II and Si II resonant transitions. In a cool gas outflow, each C II absorption should be balanced by C II or C II* emission into a random direction. We will therefore observe the wind component along our LOS in C II absorption, with weaker C II* emission. However, neutral gas outside of the LOS to the central starburst will also absorb far-UV photons and emit some of the resulting C II and C II* photons into our LOS. This emission from other parts of the wind should partially fill in the C II absorption and strengthen the C II* emission. *Therefore, the C*II *absorption and fluorescent C*II* *emission probe the outflow geometry and optical depth.*

The lack of C II absorption and the presence of C II* emission in J0816+22 and J1219+15 resemble the Prochaska et al. (2011) model for an unobscured UV emission source. In this case, neutral gas located *outside* the LOS to the starburst absorbs UV radiation and emits C II* photons *into* our LOS. C II λ1334.5 emission should be weaker than C II* λ1335.7 due to its lower transition probability and higher chance of absorption. As discussed previously, the Lyα profiles of J0816+22 and J1219+15 also suggest minimal absorption along the LOS, as expected for a mostly unobscured source.

J0303-08 shows broad, blue-shifted C II absorption, but no C II* emission, similar to expectations for a collimated neutral outflow aligned with the LOS (Prochaska et al. 2011). Neutral, outflowing gas in front of the UV emission source will cause strong C II absorption. This gas will also produce C II* emission, but as the gas will emit isotropically, most of the emission will be directed away from our LOS. The weakness of the C II* emission in J0303-08 would then imply a lack of neutral material outside of the outflow. A high dust optical depth could also suppress the C II* emission (Prochaska et al. 2011), but the Balmer decrement implies a low extinction in J0303-08 (Jaskot & Oey 2013). Alternatively, given the larger spatial extent of J0303-08, the C II*-emitting material may be located at large radii. The COS aperture might not encompass this emission, or the lower resolution at large radii may weaken its detectability. Imaging observations may determine whether neutral gas exists outside our LOS. Regardless, the C II absorption, deep, blue-shifted Lyα absorption trough, and weak Lyα emission in J0303-08 are consistent with an optically thick, neutral outflow along the LOS.

While the strongest LAEs (J0816+22 and J1219+15) show C II* emission, the strongest non-resonant emission lines appear in the weakest LAE, J1457+22. This C II* detection is unexpected, given the trends with C II* and Lyα strength in stacked spectra, and demonstrates that stacked spectra may not match the real spectra of individual objects. A dense ISM component along the LOS will produce strong C II absorption and C II* emission near the systemic velocity (Prochaska et al. 2011), as seen in J1457+22. This scenario fits with our earlier conjecture that J1457+22 is highly inclined to our LOS. The high column density of the absorbing material results in a high optical depth to C II photons, suppressing their emission, while producing a large supply of C II* photons that escape. This deep column of neutral gas naturally explains the broad Lyα absorption, while the weak, superimposed Lyα emission may escape from scattering in a bipolar outflow.

3. DISCUSSION

The geometry of the neutral ISM and its line-of-sight optical depth lead to a close connection between Lyα emission, C II and Si II absorption, and C II* and Si II* emission. Previous studies of stacked spectra of LAEs have found that higher Lyα EWs correlate with weaker interstellar absorption lines and stronger Si II* emission (e.g., Shapley et al. 2003; Berry et al. 2012). The weak absorption lines may indicate that stronger LAEs have lower LyC optical depths (Shapley et al. 2003). In our spectra of individual GPs, we likewise find that the two GPs with the strongest Lyα emission may be optically thin to the LyC. Since most of their neutral gas is not located along the LOS to the central starburst, we observe fluorescent C II* and Si II* emission with no accompanying C II and Si II absorption. This geometry may account for the similar Si II* emission observed in stacked LAE spectra. The two GPs with weaker Lyα emission do appear to have significant neutral gas in front of the starburst, but they differ in their inclinations and geometry. As a result, while both galaxies have C II and Si II absorption, only the more inclined GP shows strong C II* and Si II* emission. J0303-08 either lacks neutral material to the side, has high extinction, or has neutral material only at large radii. A highly extended geometry would also reduce the Lyα emission in J0303-08. If strong C II absorption is ubiquitous in weak LAEs, but C II* emission depends on geometry, dust extinction, and inclination, C II absorption may appear in a stacked spectrum while the C II* emission is weakened. On the other hand, the wavelength of C II absorption depends on outflow velocity, whereas C II* emission should occur near the systemic velocity.

The Lyα emission and C II absorption in the GPs supports the hypothesis that some galaxies with high [O III]/[O II] may be LCEs. Two of the four GPs have weak C II absorption, strong Lyα emission, and Lyα profiles that resemble Balmer emission from circumstellar ejecta. These properties are consistent with a low LOS optical depth. The presence of fluorescent C II* emission suggests that these GPs do have excited neutral gas outside the LOS. Therefore, LyC emission may escape anisotropically, and identifying optically thin galaxies will depend on viewing orientation (e.g., Zastrow et al. 2011; Nestor et al. 2011). J1457+22, which appears highly inclined and optically thick along the LOS, may be optically thin in other directions; emission-line imaging may determine its transverse optical depth (e.g., Zastrow et al. 2011).

Lyα emission may be an effective diagnostic of LyC optical depth (e.g., V14). A low LyC optical depth should facilitate Lyα escape, resulting in higher Lyα EWs and Lyα line profiles that are less affected by scattering. Five of the eight $z \sim 2-3$ LAEs studied by Hashimoto et al. (2013) have peak velocities within 200 km s^{-1} of the systemic velocity, similar to J0816+22 and J1219+15, and suggestive of a low column density. The strong Lyα emission and indications of a relatively low optical depth in two GPs suggest that these galaxies are low-redshift analogs of high-redshift LAEs and LCEs.

Some high-redshift starbursts, particularly strong LAEs, may have low neutral column densities. As a result, these LAEs may show narrow Lyα profiles, indicating a reduced optical depth. C II absorption and C II* emission can probe the orientation and optical depth of neutral outflows in LAEs and, along with Lyα profile shape, can help identify candidate LCEs.

We thank the anonymous reviewer for insightful comments that substantially improved this *Letter*. We are grateful to Claus Leitherer, Sangeeta Malhotra, John Salzer, and Anne Verhamme for comments on the manuscript and to Steve Finkelstein, Alex Hagen, and Tim Heckman for helpful discussions. AEJ acknowledges support from an NSF Graduate Research Fellowship. Support was provided by NASA through grant HST-GO-13293 from STScI, which is operated by AURA under NASA contract NAS-5-26555. SDSS-III is funded by the Sloan Foundation, the Participating Institutions, NSF, and DOE.

REFERENCES

Ahn, C. P., et al. 2012, ApJS, 203, 21
Ahn, S.-H., Lee, H.-W., & Lee, H. M. 2000, Journal of Korean Astronomical Society, 33, 29
Balick, B. 1989, AJ, 97, 476
Behrens, C., Dijkstra, M., & Niemeyer, J. C. 2014, A&A, 563, A77
Berry, M., et al. 2012, ApJ, 749, 4
Bouwens, R. J., et al. 2012, ApJ, 752, L5
Brocklehurst, M. 1971, MNRAS, 153, 471
Burmeister, M., & Leedjärv, L. 2009, A&A, 504, 171
Ciardullo, R., et al. 2012, ApJ, 744, 110
Cowie, L. L., Barger, A. J., & Hu, E. M. 2010, ApJ, 711, 928
Erb, D. K., Pettini, M., Shapley, A. E., Steidel, C. C., Law, D. R., & Reddy, N. A. 2010, ApJ, 719, 1168
Finkelstein, S. L., Cohen, S. H., Malhotra, S., & Rhoads, J. E. 2009, ApJ, 700, 276
Gawiser, E., et al. 2007, ApJ, 671, 278
Giammanco, C., Beckman, J. E., & Cedrés, B. 2005, A&A, 438, 599
Giavalisco, M., Koratkar, A., & Calzetti, D. 1996, ApJ, 466, 831
Hagen, A., et al. 2014, ApJ, 786, 59
Hashimoto, T., Ouchi, M., Shimasaku, K., Ono, Y., Nakajima, K., Rauch, M., Lee, J., & Okamura, S. 2013, ApJ, 765, 70
Hayes, M., Schaerer, D., Östlin, G., Mas-Hesse, J. M., Atek, H., & Kunth, D. 2011, ApJ, 730, 8
Hayes, M., et al. 2013, ApJ, 765, L27
Heckman, T. M., Sembach, K. R., Meurer, G. R., Leitherer, C., Calzetti, D., & Martin, C. L. 2001, ApJ, 558, 56
Ivison, R. J., Bode, M. F., & Meaburn, J. 1994, A&AS, 103, 201
Iwata, I., et al. 2009, ApJ, 692, 1287
Izotov, Y. I., Guseva, N. G., & Thuan, T. X. 2011, ApJ, 728, 161
Jaskot, A. E., & Oey, M. S. 2013, ApJ, 766, 91
Kornei, K. A., Shapley, A. E., Erb, D. K., Steidel, C. C., Reddy, N. A., Pettini, M., & Bogosavljević, M. 2010, ApJ, 711, 693
Kunth, D., Mas-Hesse, J. M., Terlevich, E., Terlevich, R., Lequeux, J., & Fall, S. M. 1998, A&A, 334, 11
Lee, H.-W. 2000, ApJ, 541, L25
Leitet, E., Bergvall, N., Hayes, M., Linné, S., & Zackrisson, E. 2013, A&A, 553, A106
Leitherer, C., Ferguson, H. C., Heckman, T. M., & Lowenthal, J. D. 1995, ApJ, 454, L19
Malhotra, S., Rhoads, J. E., Finkelstein, S. L., Hathi, N., Nilsson, K., McLinden, E., & Pirzkal, N. 2012, ApJ, 750, L36
Nakajima, K., & Ouchi, M. 2013, ArXiv e-prints
Nestor, D. B., Shapley, A. E., Kornei, K. A., Steidel, C. C., & Siana, B. 2013, ApJ, 765, 47
Nestor, D. B., Shapley, A. E., Steidel, C. C., & Siana, B. 2011, ApJ, 736, 18
Nota, A., Smith, L., Pasquali, A., Clampin, M., & Stroud, M. 1997, ApJ, 486, 338

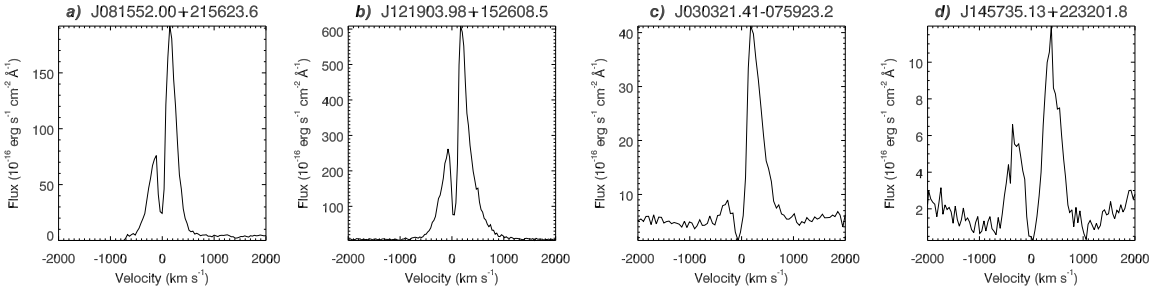

FIG. 1.— Lyα emission in the four GPs.

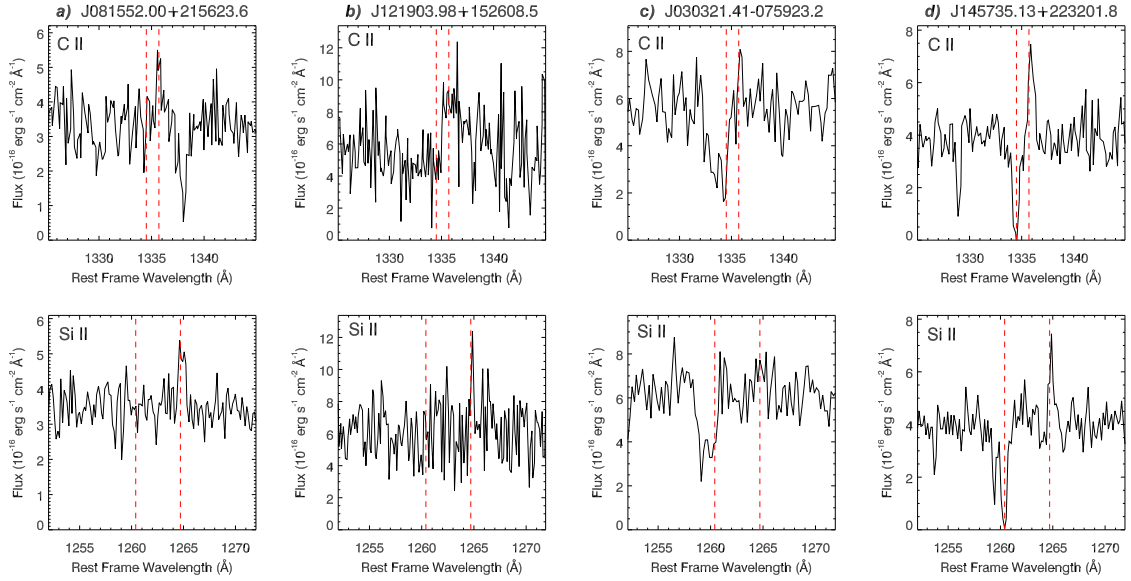

FIG. 2.— Top panels: C II λ1334.5 absorption and C II* λ1335.7 emission in the GPs. Bottom panels: Si II λ1260.4 absorption and Si II* λ1264.7 emission. Red dashed lines indicate the expected positions of these transitions from the SDSS systemic redshifts.

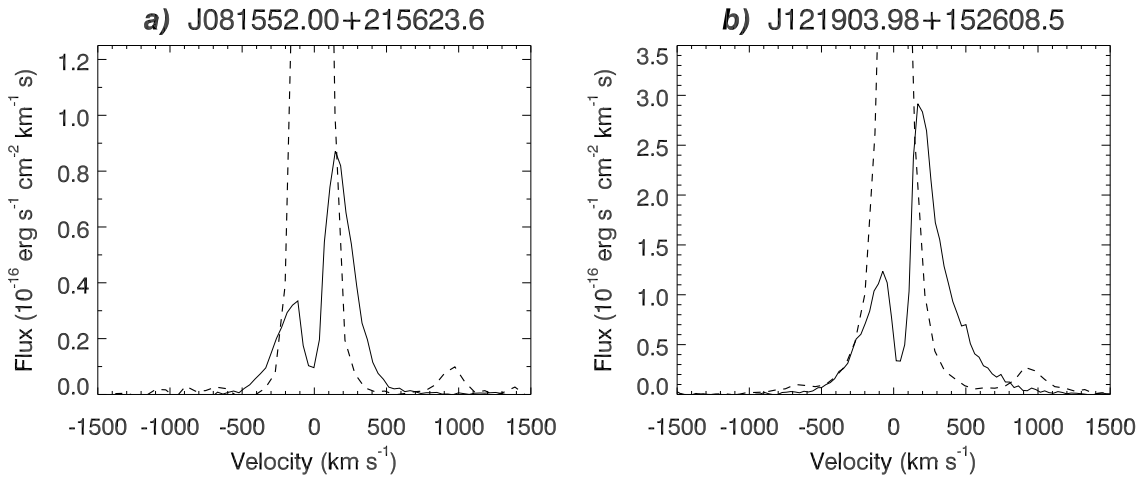

FIG. 3.— Solid lines show the Lyα emission for J0816+22 and J1219+15. Dashed lines show the Hα profiles from the SDSS spectra, scaled by a factor of 8.7 to approximate the intrinsic Lyα profiles. The [N II] lines appear as bumps near -700 and +1000 km s^{-1}.

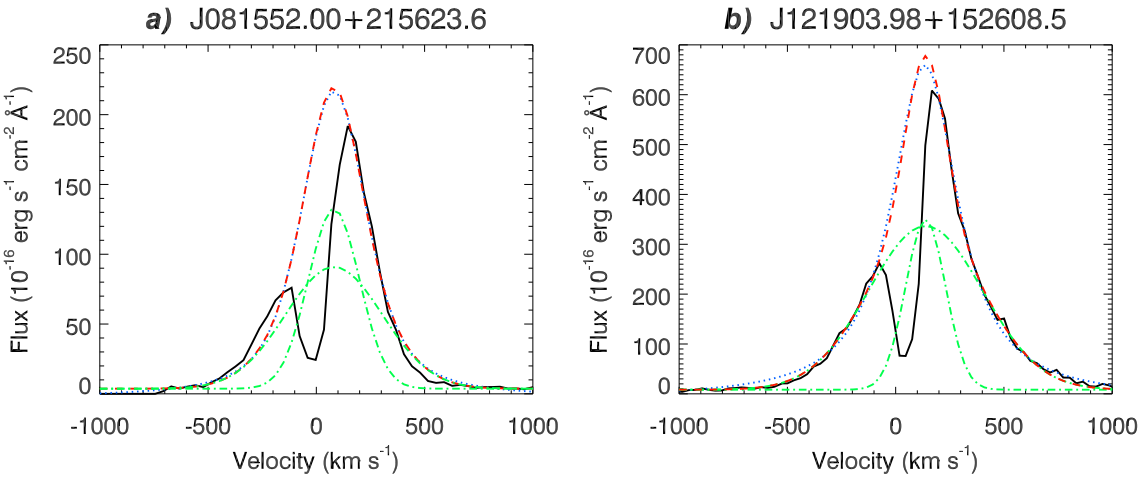

FIG. 4.— Solid lines show observed Lyα emission. Blue dotted lines indicate a Voigt fit, and red dashed lines indicate fits based on the sum of the two Gaussian components shown with green dash-dotted lines.

TABLE 1
GP UV SPECTRAL PROPERTIES

ID	z	$\frac{[\mathrm{O\,III}]}{[\mathrm{O\,II}]}$ [a]	r_{50}^{b} (kpc)	Binning (Å pix^{-1})	Lyα EW (Å)	$\Delta v_{\mathrm{peak}}^{c}$ (km s^{-1})	C II EW[d] (Å)	C II* EW[d] (Å)	Si II EW[d] (Å)	Si II* EW[d] (Å)
J081552.00 +215623.6	0.1410	13.7	0.4	0.17	71 ± 11	260	...	0.2	...	0.5
J121903.98 +152608.5	0.1956	12.4	0.5	0.15	149 ± 30	270	...	1.4	...	0.3
J030321.41 -075923.2	0.1648	9.4	0.8	0.23	9 ± 3	440	-1.3	...	-1.0	...
J145735.13 +223201.8	0.1487	9.8	0.5	0.18	-6 ± 7[e]	750	-0.9	0.7	-0.9	0.3

[a] [O III] $\lambda\lambda$5007,4959/[O II] λ3727 from Jaskot & Oey (2013).
[b] NUV half-light radius.
[c] Separation of Lyα peaks.
[d] Based on Gaussian fits.
[e] The surrounding absorption trough causes the negative EW.

Orsi, A., Lacey, C. G., & Baugh, C. M. 2012, MNRAS, 425, 87
Pellegrini, E. W., Oey, M. S., Winkler, P. F., Points, S. D., Smith, R. C., Jaskot, A. E., & Zastrow, J. 2012, ApJ, 755, 40
Petrosian, V. 1976, ApJ, 209, L1
Prochaska, J. X., Kasen, D., & Rubin, K. 2011, ApJ, 734, 24
Quiroga, C., Mikołajewska, J., Brandi, E., Ferrer, O., & García, L. 2002, A&A, 387, 139
Sánchez Contreras, C., Sahai, R., Gil de Paz, A., & Goodrich, R. 2008, ApJS, 179, 166
Shapley, A. E., Steidel, C. C., Pettini, M., & Adelberger, K. L. 2003, ApJ, 588, 65
Thuan, T. X., & Izotov, Y. I. 1997, ApJ, 489, 623
Vanzella, E., Siana, B., Cristiani, S., & Nonino, M. 2010, MNRAS, 404, 1672
Verhamme, A., Dubois, Y., Blaizot, J., Garel, T., Bacon, R., Devriendt, J., Guiderdoni, B., & Slyz, A. 2012, A&A, 546, A111
Verhamme, A., Orlitova, I., Schaerer, D., & Hayes, M. 2014, ArXiv e-prints
Verhamme, A., Schaerer, D., & Maselli, A. 2006, A&A, 460, 397
Weis, K. 2003, A&A, 408, 205
Zastrow, J., Oey, M. S., Veilleux, S., McDonald, M., & Martin, C. L. 2011, ApJ, 741, L17
Zheng, Z., & Miralda-Escudé, J. 2002, ApJ, 578, 33